Theor Chem Acc (2004) 112: 16–26
DOI 10.1007/s00214-003-0557-9

Theoretical
Chemistry Accounts

Regular article

A systematic theoretical investigation of the lowest valence- and Rydberg-excited singlet states of *trans-butadiene*. *The character of the* 1^1B_u (V) state revisited

Michal Dallos, Hans Lischka

Institute for Theoretical Chemistry and Structural Biology, University of Vienna,
Währingerstrasse 17, 1090 Vienna, Austria

Received: 18 June 2003 / Accepted: 11 August 2003 / Published online: 24 February 2004

Abstract. In the present work systematic procedures for the balanced description of the lowest singlet excited valence and Rydberg states of butadiene, especially for the correct description of the 1^1B_u state, are presented. In the first step of the calculation averaged natural orbitals (ANOs) were computed from the density matrices of the ground state, the 2^1A_g and the 1^1B_u states. For the 1^1B_u state the configuration interaction (CI) wave function used for the computation of the respective density matrix contained all possible single and double excitations from the $1b_g(\pi)$ orbital into all virtual orbitals and double excitations describing σ–π electron correlation. For the ground and 2^1A_g states a standard multireference (MR) CI with singles and doubles (CISD)/complete-active-space (CAS)(4,4) wave function was used. In the second step, these ANOs were used in extended MR-CISD, MR-CISD with Davidson correction and MR averaged quadratic coupled cluster calculations. This scheme was also extended to state-averaging including the four lowest Rydberg states $1^1B_g(3s)$, $1^1A_u(3p_\sigma)$, $2^1A_u(3p_\sigma)$ and $2^1B_u(3p_\pi)$. Our best value for the vertical excitation energy to the 1^1B_u state is 6.18 eV, close to previous equation-of-motion coupled-cluster with singles and doubles including noniterative triples [EOM – CCSD$(\tilde{T})$] and complete-active-space perturbation theory to second order (CASPT2) results, but significantly lower than most of the previous MR-CI and MR-CI based results. The computed vertical excitation energy to the 2^1A_g state of 6.55 eV is significantly below previous EOM-CCSD(T) and EOM – CCSD$(\tilde{T})$ results and demonstrates the deficiencies of these methods in the case of MR situations. On the other hand, this excitation energy is larger than previous CASPT2 results for the 2^1A_g state. The character of the 1^1B_u state is predominantly of valence character, but is more diffuse than the ground state. $<x^2>$ values for the 1^1B_u state range between 25.4 and 26.3a_0^2 in the three-state calculations.

Correspondence to: H. Lischka
e-mail: hans.lischka@univie.ac.at

Keywords: Rydberg and valence states – Ab initio multireference calculations – Multireference configuration interaction with singles and doubles and multireference averaged quadratic coupled cluster – Valence character of the 1^1B_u state

Introduction

The lowest excited valence singlet states of butadiene are the 1^1B_u and 2^1A_g states. Their understanding and description is still a challenging problem for experimentalists as well as for theoreticians. The 1^1B_u state has been observed experimentally by UV and electron impact studies, giving a system of broad absorption bands between 5.7 and 6.3 eV [1, 2, 3]. The intensity maximum occurs at 5.92 eV. The transition to the 2^1A_g state is dipole-forbidden. For octatetraene and higher polyenes the 2^1A_g state is found to be lower than the 1^1B_u state [4]. Especially for butadiene the relative ordering of these two states still remains unclear. From resonance Raman spectra it has been concluded [5] that the 2^1A_g state is located below the 1^1B_u state between 5.4 and 5.8 eV while electron impact studies [3, 6] have been interpreted such that a reverse ordering is found with a $^1A_g \rightarrow {}^1A_g$ transition centered at 7.4 eV. The 2^1A_g state is expected to play a crucial role for the photochemistry of butadiene because of a conical intersection with the 1^1B_u state (Refs. [7, 8], and references therein). The Rydberg states have been characterized experimentally as well [1, 2, 3, 9].

A great variety of methods have been used for theoretical investigations on electronic excitations in *trans*-butadiene. Vertical excitation energies have been computed by Watts et al. [10] using the equation-of-motion coupled-cluster with singles and doubles including noniterative triples [EOM-CCSD(T) and EOM – CCSD$(\tilde{T})$] methods. Especially, the vertical

excitation energy of 6.13 eV [EOM − CCSD$(\tilde{T})$] for the 1^1B_u state is quite close to the experimentally observed band maximum of 5.92 eV. However, the 2^1A_g state is probably located too high in energy since the EOM method cannot treat the multireference (MR) character of this state adequately. Good results have also been obtained by complete-active-space perturbation theory to second order (CASPT2) calculations performed by Serrano-Andrés et al. [11] and Ostojić and Domcke [7]. In both cases the 2^1A_g state is located much lower in comparison to the aforementioned EOM calculations. With a vertical excitation energy of 6.27 eV it is situated only slightly above the 1^1B_u state (6.06 [7] and 6.23 eV [11]).

A large number of calculations have been performed using the MR configuration interaction with singles and doubles interactions (CISD) method [12, 13, 14, 15, 16, 17, 18]. Standard MR-CISD calculations frequently encounter the difficulty to describe the character of the 1^1B_u state correctly. A typical situation observed in MR-CISD calculations is an artificial valence–Rydberg mixing between the 1^1B_u(V) and $2^1B_u(3p_\pi)$ states [11, 16]. Moreover, the calculated excitation energy for the 1^1B_u state is usually too high. Using MR-CI approaches with various selection schemes, the question of the character of the 1^1B_u state has been studied extensively by Cave and Davidson [16]. Further investigations on the valence–Rydberg mixing have been carried out by Cave [19] using Davidson-corrected CI calculations and quasi-degenerate variational perturbation theory (QDVPT). The importance of size-inconsistency effects was been stressed in that work. The excitation to the 2^1A_g state has been studied systematically by Lappe and Cave [20] using a variety of methods such as selected CI including Davidson corrections, QDVPT, CASPT2 and CCSD(T) methods. Recently, Cabrero et al. [21] used the Davidson correction in connection with a difference-dedicated CI scheme. Symmetry-adapted-cluster CI [22] has been applied as well. For comparison a selected set of results available in the literature is presented in Table 1.

From the work of Cave and Davidson [16] and Cave [19] the 1^1B_u state appears to be significantly more diffuse than a normal valence state. Corresponding excitation energies are relatively insensitive to the character of the wave function. A more compact character of the 1^1B_u state has been found by Watts et al. [10] in EOM-CCSD calculations. No ambiguities exist concerning the character of the 2^1A_g state. It is of valence character and possesses a genuine MR wave function [12] as opposed to the 1^1B_u state, which is of single-reference type.

The difficulties encountered with the calculation of the 1^1B_u state of butadiene are very similar to those discussed in the work of McMurchie and Davidson [23], Davidson [24] and Müller et al. [25] for the 1^1B_{1u}(V) state of ethylene. In Refs. [23, 24] differential electron correlation effects on excitation to the 1^1B_{1u} state were investigated and the importance of "complete spaces" with respect to the π orbitals and of σ–π correlation for a proper description of the V state was stressed. These ideas have been used by Müller et al. [25] to develop a two-step procedure for MR calculations. In the first step a CI calculation including differential electron correlation effects according to the aforementioned principles giving practically invariant energies and $<x^2>$ expectation values with respect to the initial set of molecular orbitals (MOs) was performed. In the second step, the natural orbitals (NOs) resulting from this initial CI were used for extensive MR-CISD and MR averaged quadratic coupled cluster (AQCC) [26, 27] calculations with the aim of computing total electron correlation energies as accurately as possible.

The goal of the present work was to extend the approach of Müller et al. [25] to calculations on excited states of butadiene and to develop a generalized and stable orbital generation scheme for the lowest excited singlet states of butadiene. Even though in this investigation only vertical excitations are considered, our investigations aim also at future work describing larger sections of potential-energy surfaces including conical intersections. These considerations motivated us to use genuine MR methods such as MR-CISD and MR-AQCC. The advantage of the latter method is that size-extensivity corrections are included in an a priori way and allow the calculation of analytic gradients [28, 29, 30]. Besides the larger size of butadiene in comparison with ethylene the situation is more complicated because the valence-excited 2^1A_g state also needs to be considered. Moreover, we wanted to include several Rydberg states as compared with the single Rydberg state considered in Ref. [25]. A common orbital set will be generated from a specially designed CI constructed in a similar way as described previously for ethylene. The NOs obtained in this CI procedure are used for the final calculations carried out at the MR-CISD, MR-CISD with Davidson correction (MR-CISD + Q) [31, 32] and

Table 1. Experimental and calculated excitation energies (eV) for the lowest valence and Rydberg states of butadiene

	EOM-CCSD(T)	EOM − CCSD$(\tilde{T})$	CASPT2	CASPT2	QDVPT	MR-CISD	MR-CISD	MR-CCCI-PS	Exp.
Reference	[10]	[10]	[11]	[7]	[19]	[17]	[16]	[18]	
1^1B_u(V)	6.36	6.13	6.23	6.06	6.39	6.70	6.2[a]	6.48	5.92 [1]
$1^1B_g(3s)$	6.36	6.19	6.29						6.20 [9],6.22 [2]
2^1A_g	6.92	6.76	6.27	6.27		6.78	6.2–6.8	6.53	
$1^1A_u(3p_\sigma)$	6.57	6.41	6.56						6.66 [2, 3]
$2^1A_u(3p_\sigma)$	6.72	6.56	6.69						
$2^1B_u(3p_\pi)$	7.22	7.03	6.70						7.07 [2,3]

[a]Recommended value

MR-AQCC levels. First we focus in our work on the electronic ground state and the two lowest valence excited states, 1^1B_u and 2^1A_g. After the successful construction of one common orbital set, which is balanced for these three states, we extend our calculations by adding the lowest excited $1^1B_g(3s)$, $1^1A_u(3p_\sigma)$, $2^1A_u(3p_\sigma)$ and $2^1B_u(3p_\pi)$ Rydberg states.

Computational details

Two series of calculations on the excited states of butadiene were performed. In the first set we included the ground state 1^1A_g, the 2^1A_g and the 1^1B_u valence states only. In the second set the Rydberg states $1^1B_g(3s)$, $1^1A_u(3p_\sigma)$, $2^1A_u(3p_\sigma)$ and $2^1B_u(3p_\pi)$ were added, so that in total seven states were taken into account. In the case of calculating the valence states only, modified augmented correlation-consistent double-zeta and triple-zeta basis sets (aug-cc-pVDZ and aug-cc-pVTZ) [33, 34] were used. For reasons of economy the augmented functions were restricted to the s and p set on carbon. This extension aimed mainly at the improvement of the description of the π system. For hydrogen the standard correlation-consistent basis sets without augmented functions were used. These basis sets were still compact enough to allow the selection of extended reference wave functions. They are denominated aug′-cc-pVDZ and aug′-cc-pVTZ. For calculations including the Rydberg states diffuse s and p functions from the doubly (d-) augmented basis [35, 36] were added to the singly augmented basis. In the d-aug′-cc-pVDZ basis set the full aug-cc-pVDZ(s,p,d) on carbon augmented by the d-aug diffuse s and p set was used. On hydrogen the cc-pVDZ basis was combined with augmented and d-augmented s functions. The d-aug′-cc-pVTZ basis contained the cc-pVTZ basis plus augmented s, p and d functions and d-augmented s and p functions on carbon. On hydrogen the aug-cc-pVTZ basis excluding the diffuse d function was used. The construction of MOs and of the space of configuration state functions (CSFs) is described in the following subsections. Using these MOs MR-CISD calculations [37] combined with the extended Davidson correction [31, 32] and MR-AQCC calculations [26, 27] were performed. All calculations refer to vertical excitations calculated at the experimental geometry [38] using C_{2h} symmetry. The molecule is located in the *yz*-plane. In all post-multiconfigurational self-consistent-field (MCSCF) methods the 1*s* core orbitals of carbon were kept frozen. The calculations were carried out using the COLUMBUS quantum chemical program package [39, 40, 41, 42] including the recently developed parallel MR-CISD/MR-AQCC program (Ref. [43] and T. Müller, H. Lischka unpublished work). The atomic orbital integrals were computed with program modules taken from DALTON [44].

Generation of orbitals

As already mentioned in the Introduction, the most problematic case is the 1^1B_u state because the valence character of the $2a_u(\pi^*)$ orbital may depend significantly on the method of calculation (see later). In order to devise a stable set of steps for the construction of the butadiene MOs for the 1^1B_u state we follow the ideas and procedures developed in the investigations of McMurchie and Davidson [23], Davidson [24] and Müller et al. [25] already described in the Introduction. At the beginning a single-state CASSCF(4,4) calculation was performed for this state with the four electrons distributed in the four π orbitals ($1a_u$, $1b_g$, $2a_u$ and $2b_g$). For the CI calculations of the next step we used as reference wave functions a CAS for two electrons and as active orbitals the $\pi(1b_g)$ orbital together with *n* orbitals of a_u symmetry. Starting with the $2a_u$ orbital *n* was consecutively increased to cover all a_u orbitals available in the given basis. The $1a_u$ orbital was always kept doubly occupied as a reference. The increasing number of a_u orbitals should give adequate flexibility for the determination of a final $2a_u(\pi^*)$ orbital. Based on this reference wave functions up to double excitations were allowed in the following way: (1) single excitations from all reference doubly occupied (DOCC) and CAS orbitals; (2) double excitations from the CAS (π) orbitals; (3) double excitations where one electron comes from one of the DOCC orbitals (σ and $1a_u$) and the second one from one of the CAS orbitals (π) (Fig. 1a). We denote these calculations as CISD($\sigma\pi$-corr). In the next step one joint set of orbitals was generated for the three lowest valence states by computing averaged NOs (ANOs) from the one-particle density matrix averaged over the 1^1A_g, 2^1A_g and 1^1B_u states. For the 1^1B_u state the density matrix of the CISD($\sigma\pi$-corr) calculation was used. For the 1^1A_g and 2^1A_g states a state-averaged (SA) CASSCF(4,4) (equal weights) calculation was performed followed by a MR-CISD calculation using the same CAS(4,4) reference space.

In the final step, the simultaneous calculation of the three lowest singlet valence states (1^1A_g, 1^1B_u and 2^1A_g) and of the four lowest singlet Rydberg states [$1^1B_g(3s)$, $1^1A_u(3p_\sigma)$, $2^1A_u(3p_\sigma)$ and $2^1B_u(3p_\pi)$], a similar scheme as in the previous case was used. First a SA-MCSCF (equal weights) for all seven states was performed. The active space consisted of the CAS(4,4) plus individual Rydberg

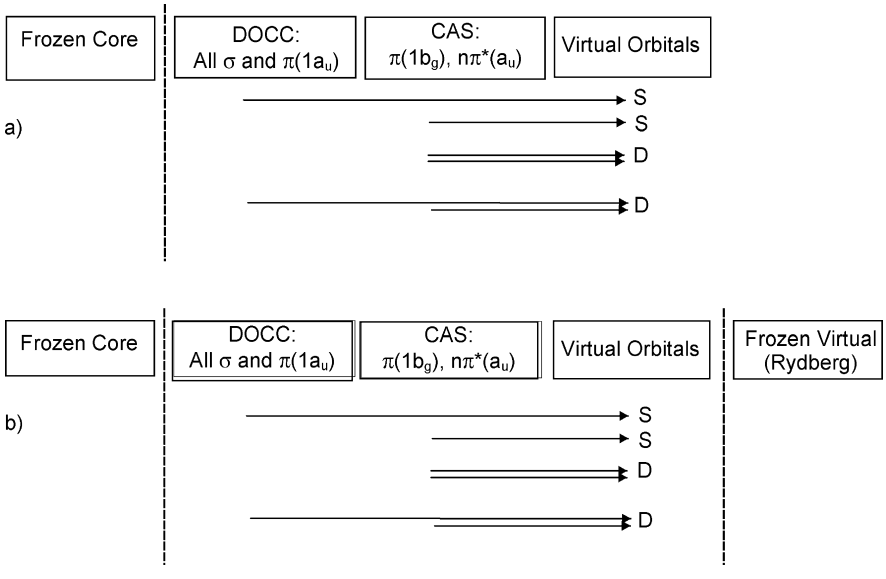

Fig. 1. Characterization of the CISD($\sigma\pi$-corr) scheme: **a** three-state case, **b** seven-state case including Rydberg states. *S* denotes single excitations and *D* denotes double excitations

configurations. The purpose of this calculation was to obtain optimized Rydberg orbitals. Using this orbital set a CISD($\sigma\pi$-corr) calculation for the 1^1B_u state and a MR-CISD calculation in a CAS(4,4) for the 1^1A_g and 2^1A_g states was performed, in which the four Rydberg orbitals were kept frozen in the form obtained in the SA-MCSCF calculation (Fig. 1b). To obtain the final set of orbitals we again computed the ANOs from the one-particle density matrix averaged over the 1^1A_g, 2^1A_g and 1^1B_u states.

Final calculations

The final calculations were performed at the MR-CISD, MR-CISD + Q and MR-AQCC levels using the ANOs as described in the previous subsection and a variety of reference spaces. For the investigations on the three valence states the smallest reference space was CAS(4,4). The next one was generated by extending the CAS(4,4) space by the $3a_u$ orbital. We denote this reference space as CAS(4,5). Further reference spaces were constructed by including σ orbitals into the active space. Including all these orbitals into a CAS would have resulted in total CSF expansion spaces that were too large; therefore, systematic reduction schemes were used in order to keep the CSF dimensions manageable. The RCA1 reference space was constructed by adding to the CAS(4,4) space three originally doubly occupied orbitals into a restricted active space (RAS) and four former virtual orbitals into an auxiliary space (AUX). The reference configurations were generated within this orbital set by allowing single excitations from the RAS orbitals and single excitations into the AUX orbitals. By further enlarging the RAS and AUX spaces we generated the RCA2 and RCA3 reference spaces. The composition of these orbital spaces and the resulting sizes of the total CSF expansion spaces are summarized in Table 2.

For the calculations including the Rydberg states similar reference spaces were used. Here the smallest reference space consisted of the CAS(4,4) space plus the individual Rydberg configurations of the given symmetry. We denote this space as CAS(4,4 + R). In the next step we allowed all reference single excitations from the reference CAS orbitals into the Rydberg orbitals and denote this space as CAS(4,4 + R1ex). Finally we included the $3a_u$ orbital into the CAS and obtained the CAS(4,5 + R1ex) reference space.

Allowing all single and double excitations at the orbital occupation level from all reference configurations into all virtual orbitals generated the final CSF expansion set. The full single- and double-excited CSF expansion space was constructed by using reference configurations of all symmetries. Depending on the denomination of the starting reference space we denote theses calculations using an additional label F (e.g. CAS(4,4)-F). As a second possibility, excitations from reference configurations with the spatial symmetry equal to the symmetry of the calculated state were constructed only and the single- and double-expansion space was restricted to the interacting space [45]. These calculations are denoted by an additional R. In the case of the MR-AQCC calculations few, additional configurations not included in the reference space ("intruder states") were observed. These intruder states consisted of excitations into the external space. In order to avoid these intruder states, the diagonal shift of the AQCC method was not applied to configurations containing these orbitals. For the extended reference spaces RCA1–RCA3, MR-AQCC did not always converge; therefore, MR-AQCC results are not given in these cases.

Results and discussion

"Conventional" CI calculations

In this subsection the difficulties encountered by conventional CI approaches for the calculation of the 1^1B_u state of butadiene are discussed. Results for different types of calculations are collected in Table 3. The aug′-cc-pVDZ and d-aug′-cc-pVDZ basis sets and various numbers of states included in the SA-CASSCF were used. In the case of single-state CASSCF calculations one finds from the $<x^2>$ expectation values that the nature of the 1^1B_u state depends significantly on the basis set. For the smaller and more compact basis set we obtained a valencelike state with an $<x^2>^{CI}$ value of $31.9a_0^2$, while for the larger basis set we found a

Table 2. Description of the reference spaces used in the MR-CISD and MR-AQCC calculations and the total numbers of configuration state functions (*CSFs*) for the ^1A_g states

Reference space descriptions	a_g	b_u	a_u	b_g	Total number of CSFs (in millions) aug′-cc-pVDZ R/F[a]	aug′-cc-pVTZ R/F[a]
CAS(4,4)					1.7/4.1	9.3/21.9
DOCC	5	4	0	0		
CAS	0	0	2	2		
CAS(4,5)					4.1/11.1	22.2/59.2
DOCC	5	4	0	0		
CAS	0	0	3	2		
RCA1					37.6/98.2	205.7
DOCC	3	3	0	0		
RAS (1ex)	2	1	0	0		
CAS	0	0	2	2		
AUX (1ex)	2	1	1	0		
RCA2					54.4/166.4	
DOCC	3	3	0	0		
RAS (1ex)	2	1	0	0		
CAS	0	0	2	2		
AUX (1ex)	2	2	2	2		
RCA3					81.6/203.3	
DOCC	2	2	0	0		
RAS (1ex)	3	2	0	0		
CAS	0	0	2	2		
AUX (1ex)	2	2	2	2		

[a]For definition see text

Table 3. Dependence of the total energies (au), excitation energies (eV) and $< x^2 >$ values (a_0^2) calculated at the CASSCF(4,4) and MR-CISD/CAS(4,4) levels on the MCSCF state-averaging procedure and basis set

State	E^{MCSCF}[a]	$\Delta E^{\mathrm{MCSCF}}$	$< x^2 >^{\mathrm{MC}}$	$E^{\mathrm{MR\text{-}CISD}}$[a]	$E^{\mathrm{MR\text{-}CISD+Q}}$[a]	$\Delta E^{\mathrm{MR\text{-}CISD}}$	$\Delta E^{\mathrm{MR\text{-}CISD+Q}}$	$< x^2 >^{\mathrm{CI}}$
aug′-cc-pVDZ, no MCSCF state-averaging								
1^1A_g	0.989636	–	21.72	1.458169	1.521872	0	0	21.8
1^1B_u	0.704033	7.77	32.80	1.196294	1.271350	7.13	6.82	31.9
d-aug′-cc-pVDZ, no MCSCF state-averaging								
1^1A_g	0.992610	–	21.75	1.473265	1.539821	0	0	21.9
1^1B_u	0.726484	7.24	74.45	1.213126	1.284892	7.08	6.94	72.8
aug′-cc-pVDZ, MCSCF state-averaging of $1^1A_g + 1^1B_u + 2^1A_g$								
1^1A_g	0.980131	–	22.04	1.454445	1.519750	0	0	21.9
1^1B_u	0.679400	8.18	22.54	1.193254	1.272931	7.11	6.72	23.0
2^1A_g	0.735263	6.66	22.52	1.206501	1.273172	6.75	6.71	22.3
d-aug′-cc-pVDZ, MCSCF state-averaging of $1^1A_g + 2^1A_g + 1^1B_u$								
1^1A_g	0.982802	–	22.07	1.469450	1.537681	0	0	22.0
1^1B_u	0.683300	8.15	22.53	1.210659	1.294256	7.04	6.62	22.9
2^1A_g	0.737731	6.67	22.51	1.221686	1.291630	6.74	6.70	22.3
d-aug′-cc-pVDZ, MCSCF state-averaging of $1^1A_g + 2^1A_g + 1^1B_u + 2^1B_u$[b]								
1^1A_g	0.981197	–	21.69	1.468878	1.537533	0	0	21.8
1^1B_u	0.736784	6.65	77.77	1.221631	1.291598	6.73	6.69	53.9
2^1A_g	0.737699	6.63	22.19	1.223520	1.297573	6.68	6.53	22.2
2^1B_u	0.676316	8.30	27.61	1.196972	1.274483	7.40	7.16	50.8

[a]Total energies given as $-(E+154)$
[b]Additional single excitations into the $3a_u$ orbital were included into the reference space in order to describe the $3p_\pi$ Rydberg state

Rydberg-like state with $< x^2 >^{\mathrm{CI}} = 72.8 a_0^2$. In the case of CASSCF state-averaging over the 1^1A_g, 2^1A_g and 1^1B_u states we got a similar result for both basis sets: the 1^1B_u state possesses valencelike character in either case. We also note that the MR-CISD method does not change the character of the 1^1B_u state as compared with the CASSCF result. The situation changes when we include the $2^1B_u(3p_\pi)$ state into the calculation. From Table 3 it is seen that at the CASSCF level the lower of the B_u states has Rydberg character ($< x^2 > = 77.8 a_0^2$) and the higher one is a valencelike state ($< x^2 > = 27.6 a_0^2$). At the MR-CISD level the two B_u states are mixed and undistinguishable in terms of $< x^2 >$, with $< x^2 >$ values of about $50 a_0^2$. These calculations demonstrate the arbitrariness of the CASSCF(4,4)-based calculations and MR-CISD results built on top of them. We see that the results strongly depend on the basis set as well as on the number and the nature of the states included into the state-averaging.

Orbital generation

The stability of the orbital generation procedure CISD($\sigma\pi$-corr) is documented in two series of calculations performed with the aug′-cc-pVDZ and d-aug′-cc-pVDZ basis sets. The dependence of the character of the 1^1B_u state as a function of the number of a_u orbitals, n, included in the reference wave function of the CISD($\sigma\pi$-corr) calculation is given in Table 4. The starting orbitals were generated by the single-state CAS(4,4) MCSCF calculation already documented in Table 3. For $n=1$, which is equivalent to a CAS(2,2) reference space, we obtained very different $< x^2 >$ values using the two basis sets. For the smaller basis a compact state was found and for the larger basis set a diffuse one. In particular, the result for the d-aug′-cc-pVDZ basis set is much too diffuse. The reason for this can be found in the large $< x^2 >$ value for the $\pi^*(2a_u)$ orbital. By increasing the number of a_u orbitals included in the active space of the reference wave function, the character of the $\pi^*(2a_u)$ orbital changes and the orbital becomes more and more compact, with a final value around $\langle x^2 \rangle_{2a_u} = 5.9 a_0^2$ for the d-aug′-cc-pVDZ basis. Following the trend of the $\langle x^2 \rangle_{2a_u}$ values, the total $< x^2 >$ values of the 1^1B_u state are decreasing as well. Finally, the $< x^2 >$ values computed with the two basis sets differ only by around $1 a_0^2$ ($24.9 a_0^2$ versus $25.8 a_0^2$) as compared with a difference of around $21 a_0^2$ for the CISD($\sigma\pi$-corr) calculation with $n=1$. We see that even starting from MCSCF orbitals of very different character ($< x^2 >$ values of $32.8 a_0^2$ and $74.5 a_0^2$ for the aug′-cc-pVDZ and d-aug′-cc-pVDZ basis sets, respectively, Table 3) the CISD($\sigma\pi$-corr) procedure converges smoothly to orbitals of very similar character. The same behavior was observed for the aug′-cc-pVTZ

Table 4. Dependence of the total energies (au) and $< x^2 >$ values (a_0^2) of the $2a_u$ natural orbitals and the total wave function computed for the 1^1B_u state on the number of a_u orbitals included in the reference space of the CISD ($\sigma\pi$-corr)method. Total energies given as $-(E+154)$

No. $\pi^*(a_u)$	aug′-cc-pVDZ			d-aug′-cc-pVDZ		
	E^{CI}	$\langle x^2 \rangle_{2a_u}$	$< x^2 >$	E^{CI}	$\langle x^2 \rangle_{2a_u}$	$< x^2 >$
1	0.828759	7.41	27.29	0.823773	28.79	48.16
3	0.835010	5.03	24.95	0.844900	6.10	25.98
5	0.835509	4.99	24.91	0.845394	5.96	25.85
9	0.835788	4.96	24.88	0.845688	5.91	25.79
11	0.835833	4.96	24.88	0.845884	5.88	25.76
12	0.835848	4.95	24.88	0.845953	5.87	25.75

and d-aug′-cc-pVTZ basis sets as well as for different starting MCSCF orbitals obtained from different MCSCF state-averaging schemes.

Simultaneous treatment of the 1^1A_g, 1^1B_u and 2^1A_g states

The results for the final calculations are based on the ANOs computed from the averaged density obtained from the CISD($\sigma\pi$-corr) calculation with $n=10$ for the 1^1B_u state and from separate MR-CISD/CAS(4,4) calculations for the 1^1A_g and 2^1A_g states. Total energies, excitations energies and total $<x^2>$ values are listed in Table 5 for the aug′-cc-pVDZ basis and in Table 6 for the aug′-cc-pVTZ basis. Furthermore, the excitation energies are represented graphically in Fig. 2.

The 2^1A_g state

For the smallest reference space, CAS(4,4)-R, and the aug′-cc-pVDZ basis the excitation energy is 6.76 eV. The Davidson-corrected excitation energy as well as the MR-AQCC value is 6.71 eV. The omission of the internal space restriction and allowing all reference symmetries [CAS(4,4)-F] results in a small lowering of the excitation energy by 0.01 eV for MR-CISD, 0.02 eV for MR-CISD + Q and by 0.03 eV for MR-AQCC. An increase of the reference space to CAS(4,5)-F leads to a further reduction of the excitation energy of 0.04 and 0.02 eV for MR-CISD and MR-CISD + Q, respectively, and to a decrease of 0.08 eV for MR-AQCC. The remaining reference spaces were used only at the MR-CISD and MR-CISD + Q levels. The MR-CISD + Q excitation energy is reduced further by 0.08 eV between the CAS(4,5)-F and RCA3-R reference spaces. From Table 5 and the graphical representation given in Fig. 2 we see that the series of excitation energies converges faster in case of MR-CISD. The MR-CISD + Q and MR-AQCC methods are more sensitive to the extension of the reference space: however, the RCA3-R results of the MR-CISD + Q calculations seem to be already quite well converged. The MR-CISD + Q energy differences between the RCA1-R, RCA2-R and RCA3-R results are with 0.04 and 0.02 eV, respectively, quite small, while the CI expansion dimensions increase significantly (for CI dimensions see Table 2). The RCA3-F MR-CISD + Q result is estimated to be 6.57 eV using the difference of 0.02 eV between the RCA2-R and RCA3-R

Table 5. Total energies (au), excitation energies (eV) and $<x^2>$ values (a_0^2) calculated at the MR-CISD, MR-CISD + Q and MR-AQCC levels based on averaged natural orbitals (*ANOs*) (ANOs based on a three-state calculation were used) using the aug′-cc-pVDZ basis. Total energies given as $-(E+154)$

State	E^{CI}	E^{CI+Q}	E^{AQCC}	ΔE^{CI}	ΔE^{CI+Q}	ΔE^{AQCC}	$<x^2>_{CI}$	$<x^2>_{AQCC}$
CAS(4,4)-R								
1^1A_g	0.454356	0.519897	0.525476	0	0	0	21.9	21.9
1^1B_u(V)	0.194047	0.274726	0.284784	7.08	6.67	6.55	23.3	23.7
2^1A_g	0.205910	0.273241	0.278871	6.76	6.71	6.71	22.4	22.9
CAS(4,4)-F								
1^1A_g	0.456079	0.522668	0.528794	0	0	0	21.9	21.9
1^1B_u(V)	0.198160	0.281852	0.293580	7.02	6.55	6.40	23.3	23.7
2^1A_g	0.207912	0.276687	0.283304	6.75	6.69	6.68	22.4	23.0
CAS(4,5)-R								
1^1A_g	0.456299	0.521163	0.526430	0	0	0	21.8	21.9
1^1B_u(V)	0.206856	0.281745	0.292799	6.79	6.51	6.36	26.9	27.6
2^1A_g	0.209626	0.275631	0.282762	6.71	6.68	6.63	22.00	22.53
CAS(4,5)-F								
1^1A_g	0.458424	0.524563	0.530469	0	0	0	21.8	21.9
1^1B_u(V)	0.210893	0.288682	0.300916	6.74	6.42	6.25	26.8	27.5
2^1A_g	0.211879	0.279469	0.287759	6.71	6.67	6.60	22.0	22.7
RCA1-R								
1^1A_g	0.464799	0.530655	–	0	0	–	21.8	–
1^1B_u(V)	0.220852	0.295402	–	6.64	6.40	–	25.8	–
2^1A_g	0.219038	0.286339	–	6.69	6.65	–	22.0	–
RCA1-F								
1^1A_g	0.470322	0.539427	–	0	0	–	21.8	–
1^1B_u(V)	0.227792	0.307089	–	6.60	6.32	–	25.7	–
2^1A_g	0.224532	0.295593	–	6.69	6.64	–	22.1	–
RCA2-R								
1^1A_g	0.469596	0.533911	–	0	0	–	21.8	–
1^1B_u(V)	0.228111	0.299029	–	6.57	6.39	–	25.5	–
2^1A_g	0.224179	0.290960	–	6.68	6.61	–	22.2	
RCA2-F								
1^1A_g	0.476065	0.544114	–	0	0	–	21.8	–
1^1B_u(V)	0.235766	0.311813	–	6.54	6.32	–	25.4	–
2^1A_g	0.230853	0.302093	–	6.67	6.59	–	22.3	
RCA3-R								
1^1A_g	0.472497	0.536798	–	0	0	–	21.8	–
1^1B_u(V)	0.231580	0.302687	–	6.56	6.37	–	25.4	–
2^1A_g	0.226989	0.294473	–	6.68	6.59	–	22.2	–

Table 6. Total energies (au), excitation energies (eV) and $< x^2 >$ values (a_0^2) calculated at the MR-CISD,MR-CISD + Q and MR-AQCC levels based on ANOs (ANOs based on a three-state calculation were used) using the aug′-cc-pVTZ basis. Total energies given as $-(E + 154)$

State	E^{CI}	E^{CI+Q}	E^{AQCC}	ΔE^{CI}	ΔE^{CI+Q}	ΔE^{AQCC}	$< x^2 >_{CI}$	$< x^2 >_{AQCC}$
CAS(4,4)-R								
1^1A_g	0.581903	0.660866	0.669198	0	0	0	21.7	21.7
1^1B_u(V)	0.321762	0.416748	0.432382	7.08	6.64	6.44	22.9	23.9
2^1A_g	0.334337	0.414763	0.423055	6.74	6.70	6.73	22.1	23.1
CAS(4,4)-F								
1^1A_g	0.583937	0.664192	0.673284	0	0	0	21.7	21.7
1^1B_u(V)	0.326408	0.424883	0.442194	7.01	6.51	6.29	22.9	23.4
2^1A_g	0.336719	0.418893	0.428845	6.73	6.67	6.65	22.1	23.2
CAS(4,5)-R								
1^1A_g	0.583870	0.662254	0.670267	0	0	0	21.6	21.8
1^1B_u(V)	0.334930	0.424362	0.439889	6.77	6.47	6.27	26.4	28.1
2^1A_g	0.337823	0.417115	0.427163	6.70	6.67	6.62	21.6	23.0
CAS(4,5)-F								
1^1A_g	0.586351	0.666271	0.675202	0	0	0	21.6	21.8
1^1B_u(V)	0.339485	0.432306	0.447457	6.72	6.37	6.20	26.3	27.9
2^1A_g	0.340496	0.421706	0.433013	6.69	6.66	6.59	21.8	22.5
RCA1-R								
1^1A_g	0.594003	0.673533	–	0	0	–	21.6	–
1^1B_u(V)	0.351387	0.440467	–	6.60	6.34	–	25.4	–
2^1A_g	0.348626	0.429809	–	6.68	6.63	–	21.8	–

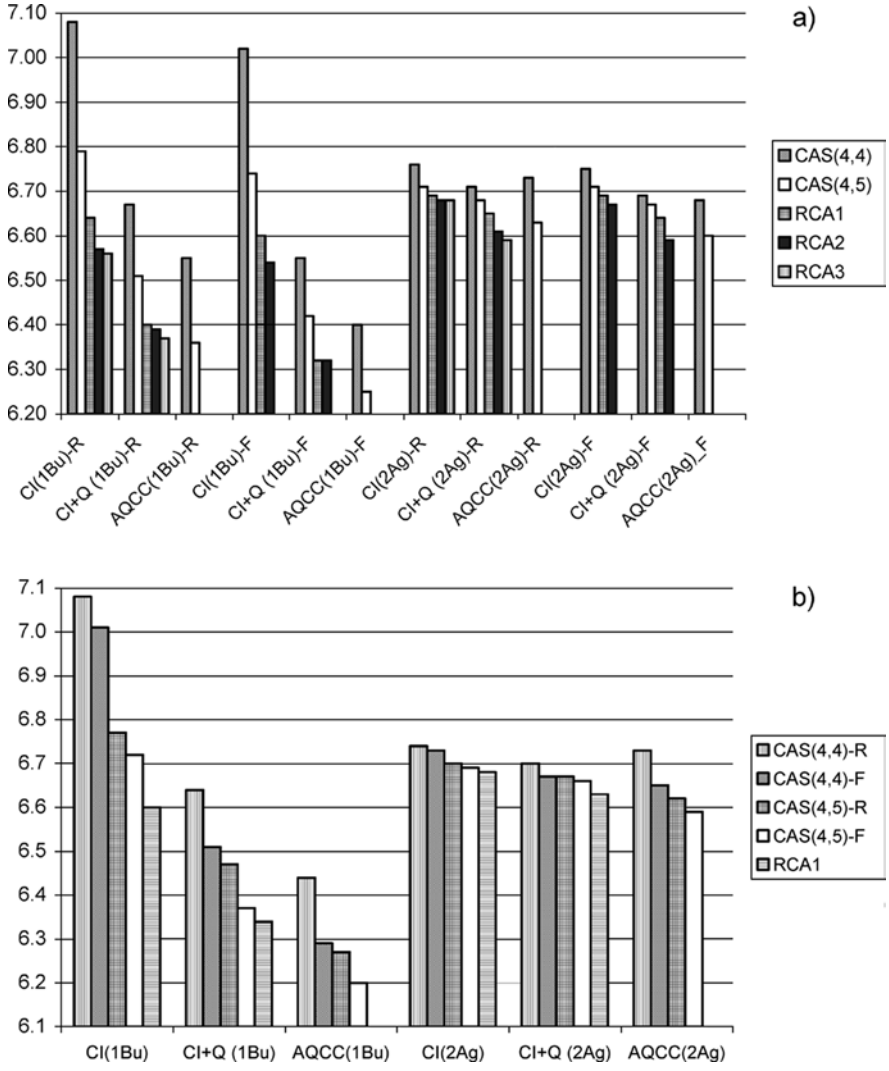

Fig. 2. Graphical representation of the excitations energies (eV) for the 1^1B_u and 2^1A_g states of butadiene: **a** aug′-cc-pVDZ basis set, **b** aug′-cc-pVTZ basis set

excitation energies. The best MR-AQCC value of 6.60 eV is quite close to the just-mentioned RCA3-F MR-CISD + Q value.

The situation is similar for the aug′-cc-pVTZ basis (Table 6). Owing to larger expansion dimensions for the triple-zeta basis we could not perform the MR-CISD/

MR-AQCC calculations up to the same high reference level as for the aug′-cc-pVDZ basis. We see that the convergence is similar to the aug′-cc-pVDZ case. Excitation energies are only slightly smaller by 0.01–0.02 eV. Reducing the previously mentioned estimate of 6.57 eV for the RCA3-F/MR-CISD + Q/aug′-cc-pVDZ calculation by 0.02 eV for the change to the triple-zeta basis, we obtained our best estimate for the vertical excitation to the 2^1A_g state as 6.55 eV. A similar procedure gives 6.58 eV on the basis of the MR-AQCC method.

Owing to the lack of direct experimental evidence a comparison with experimental values is not possible. We may compare our results with those of other theoretical works listed in Table 1. The MR-CISD results of 6.78 eV [17], the EOM-CCSD(T) value of 6.92 eV and the $\mathrm{EOM-CCSD}(\tilde{T})$ value of 6.76 eV [10] are systematically higher than our results. On the other hand, the CASPT2 results of 6.27 eV obtained in Refs. [7, 11] are lower than our value by 0.28 eV. Cave and Davidson [16] give a wide range of 6.2–6.8 eV. In a more recent work by Lappe and Cave [20] the 2^1A_g state is computed at 6.40 eV using a perturbation selected MR-CISD scheme with Davidson correction (DC-MR-CISD) and an estimated QDVPT value of 6.35 eV. Lappe and Cave noted that the CASPT2 value is located systematically below their DC-MR-CISD and QDVPT values by about 0.15–0.1 eV; however, no conclusive answer in terms of threshold extrapolation and basis set could be given. On the basis of our results we believe that the CASPT2 excitation energy of 6.27 eV is very likely too low. The excitation energy of 6.53 eV obtained by Serrano-Andrés et al. [18] using the MR consistent correlation perturbation selected CI method is close to our value.

The 1^1B_u(V) state

The vertical excitation energy of 7.08 eV as calculated by the MR-CISD method using the CAS(4,4) reference space and the aug′-cc-pVDZ basis set (Table 5) is much larger than the experimental band maximum of 5.92 eV. The situation improves after inclusion of the Davidson correction to 6.67 eV or using the MR-AQCC method to 6.55 eV. Extending the reference space by one additional $\pi^*(3a_u)$ orbital forming the CAS(4,5) reference space leads to a significant improvement of the excitation energy. The lowest value at this point is the MR-AQCC energy of 6.25 eV. From Fig. 2 we see that in case of the 1^1B_u state the convergence behavior of the excitation energies is by far not as good as for the 2^1A_g state. Size-extensivity effects computed by MR-AQCC give lower excitation energies than corresponding ones computed with the Davidson correction. The RCA1–RCA3 results appear to be relatively well converged since differences in excitation energies for these calculations amount only a few hundredths of an electronvolt. From the difference of 0.02 eV between the RCA2-R and RCA3-R results the RCA3-F value is estimated to be 6.30 eV [6.32 eV (RCA2-F)−0.02 eV]. The best MR-AQCC result is the aforementioned value of 6.25 eV of the MR-AQCC/CAS(4,5)-F calculation.

The results obtained with the aug′-cc-pVTZ basis set are collected in Table 6. Basis set effects as compared with the aug′-cc-pVDZ basis range from around 0.05 eV at the MR-CISD + Q level up to around 0.1 eV at the MR-AQCC level. They are significantly larger as compared with those for the 2^1A_g state. We regard the MR-AQCC/CAS(4,5)-F result of 6.20 eV obtained with the aug′-cc-pVTZ basis set as our best computed value. For a rough evaluation of basis set effects we use the double-zeta to triple-zeta two-point extrapolation formula $E = E_\infty + AX^{-3}$ of Halkier et al. [46] applied to total MR-AQCC energies. X is the cardinal number of the basis set ($X = 2$ for double zeta and $X = 3$ for triple zeta). This extrapolation gives for the MR-AQCC/CAS(4,5)-F case an extrapolated excitation energy of 6.18 eV. Comparing our result with other theoretical investigations (Table 1), we see that this MR-AQCC value of 6.18 eV for the excitation energy is close to the best ones so far achieved. It is significantly lower than most previous CI-based methods.

At the MR-CISD/CAS(4,4)-R/aug′-cc-pVDZ level a $<x^2>$ value of $23.3a_0^2$ is found, which changes only slightly to $23.7a_0^2$ in the corresponding MR-AQCC calculation. The $<x^2>$ value increases for the CAS(4,5) reference space by about $3a_0^2$; however, it is systematically lowered again by further increase of the reference space in the RCA series. MR-AQCC values are somewhat larger than MR-CISD results. For the aug′-cc-pVTZ basis the CAS(4,5)-F results given in Table 6 are $26.3a_0^2$ (MR-CISD) and $27.9a_0^2$ (MR-AQCC). These values show a valencelike 1^1B_u state, which is somewhat more diffuse than the ground state ($<x^2> = 21.8a_0^2$) and the 2^1A_g state ($<x^2> = 22.5a_0^2$). A 1^1B_u state of significantly more diffuse character has been computed by Cave and Davidson [16] ($41.3a_0^2$) and Cave [19] ($48.1a_0^2$). However, a more compact $<x^2>$ value of $32.7a_0^2$ and an excitation energy of 6.25 eV (CI4 + Q results) was reported in the investigations of Cave and Davidson [16] as well. Our result of a more compact 1^1B_u state is in better agreement with this latter value and with the one ($<x^2> = 31.7a_0^2$) computed in the EOM-CCSD calculations of Watts et al. [10].

Simultaneous treatment of the 1^1A_g, 1^1B_u(V), $1^1B_g(3s)$, 2^1A_g, $1^1A_u(3p_\sigma)$, $2^1A_u(3p_\sigma)$ and $2^1B_u(3p_\pi)$ states

In the next step of our investigations the simultaneous calculation of valence as well as Rydberg states was performed. In these calculations the results are discussed from the following points of view: (1) excitation energies and character of the 1^1B_u(V) and 2^1A_g(V) states in comparison to the previous three-state calculations in Sect. 3.3; (2) separation of the Rydberg and valence character between the 1^1B_u(V) and $2^1B_u(3p_\pi)$ states; and (3) excitation energies of the remaining Rydberg states.

At the MR-CISD level using the CAS(4,4 + R)-R reference space we obtained for the 1^1B_u state a somewhat lower vertical excitation energy than in the three-state case (6.83 versus 7.08 eV, Table 7). A further lowering of the excitation energy by inclusion of size-extensivity effects in the form of the Davidson correction (6.52 eV) or MR-AQCC (6.50 eV) is achieved. In the MR-CISD calculation the 1^1B_u state is more diffuse than it was the case of the three-state calculations. The 1^1B_u(V) and $2^1B_u(3p_\pi)$ states are well separated in terms of Rydberg–valence character. This picture is even more pronounced at the MR-AQCC level. The excitation energies for the Rydberg states are in this case higher than the experimental values (Table 1) by about 0.5 eV. The reason is that each Rydberg state is represented in this reference space by one configuration only.

As was already observed in the three-state calculations, the results are significantly improved by the inclusion of the $3a_u$ orbitals into the reference space. Furthermore, if we allow in the reference configurations all single excitations into the Rydberg orbitals [CAS(4,5 + R1ex)] instead of individual Rydberg configurations, the agreement of the excitation energies of the Rydberg states with experiment is significantly improved. In the CAS(4,5 + R1ex) calculations the excitation energy to the 1^1B_u state is close to the value obtained in the three-state calculations and a balanced description of the excitation energies of valence and Rydberg states was obtained. The excitation energy of 6.32 eV [MR-AQCC/CAS(4,5 + R1ex)-R value in Table 7] for the 3*s* Rydberg state is in good agreement with the measurements of McDiarmid [2] and Reddish

Table 7. Total energies (au), excitation energies (eV) and $< x^2 >$ values (a_0^2) calculated at the MR-CISD, MR-CISD + Q and MR-AQCC levels based on ANOs (ANOs based on a seven-state calculation were used) using the d-aug′-cc-pVTZ basis. Total energies given as $-(E+154)$

State	E^{CI}	E^{CI+Q}	E^{AQCC}	ΔE^{CI}	ΔE^{CI+Q}	ΔE^{AQCC}	$< x^2 >_{CI}$	$< x^2 >_{AQCC}$
CAS(4,4 + R)-R								
1^1A_g	0.575527	0.654794	0.663631	0	0	0	21.7	21.7
1^1B_u(V)	0.324546	0.415071	0.424941	6.83	6.52	6.50	35.8	20.7
$1^1B_g(3s)$	0.326404	0.410763	0.424689	6.78	6.64	6.50	42.7	40.2
2^1A_g	0.328942	0.409502	0.421095	6.71	6.67	6.60	23.0	23.2
$1^1A_u(3p_\sigma)$	0.315308	0.399771	0.414038	7.08	6.94	6.79	34.0	31.4
$2^1A_u(3p_\sigma)$	0.308583	0.392990	0.406967	7.26	7.12	6.98	38.1	35.7
$2^1B_u(3p_\pi)$	0.294772	0.382372	0.389479	7.64	7.41	7.49	72.5	84.9
CAS(4,4 + R)-F								
1^1A_g	0.577589	0.658195	0.667845	0	0	0	21.7	21.7
1^1B_u(V)	0.328151	0.421890	0.433848	6.79	6.43	6.37	33.1	16.4
$1^1B_g(3s)$	0.328818	0.415660	–	6.77	6.60	–	42.6	–
2^1A_g(V)	0.331340	0.413655	0.427641	6.70	6.65	6.54	22.9	23.5
$1^1A_u(3p_\sigma)$	0.317694	0.404672	–	7.07	6.90	–	33.5	–
$2^1A_u(3p_\sigma)$	0.310974	0.397909	–	7.26	7.08	–	38.0	–
$2^1B_u(3p_\pi)$	0.296533	0.385124	–	7.65	7.43	–	75.0	–
CAS(4,4 + R1ex)-R								
1^1A_g	0.575527	0.654794	0.663631	0	0	0	21.7	21.7
1^1B_u(V)	0.329608	0.415432	0.423863	6.69	6.51	6.52	49.4	31.7
$1^1B_g(3s)$	0.341416	0.421848	0.432262	6.37	6.34	6.30	42.7	39.7
2^1A_g	0.328942	0.409502	0.421057	6.71	6.67	6.60	22.3	23.1
$1^1A_u(3p_\sigma)$	0.330519	0.411000	0.422968	6.67	6.63	6.55	33.5	30.6
$2^1A_u(3p_\sigma)$	0.323255	0.403853	0.416289	6.86	6.83	6.73	38.0	20.7
$2^1B_u(3p_\pi)$	0.303796	0.390513	0.405604	7.39	7.19	7.02	58.9	73.0
CAS(4,4 + R1ex)-F								
1^1A_g	0.577589	0.658195	0.667845	0	0	0	21.7	21.7
1^1B_u(V)	0.333435	0.422393	–	6.64	6.42	–	47.7	–
$1^1B_g(3s)$	0.344812	0.427705	0.425641	6.33	6.27	6.59	42.6	39.3
2^1A_g	0.331340	0.413655	0.428105	6.70	6.65	6.52	22.3	24.6
$1^1A_u(3p_\sigma)$	0.333929	0.416903	0.415249	6.63	6.57	6.87	33.5	30.6
$2^1A_u(3p_\sigma)$	0.326721	0.409900	0.408356	6.83	6.76	7.06	37.9	34.6
$2^1B_u(3p_\pi)$	0.307826	0.397106	–	7.34	7.10	–	60.5	–
CAS(4,5 + R1ex)-R								
1^1A_g	0.577665	0.656502	0.665101	0	0	0	21.6	21.8
1^1B_u(V)	0.335021	0.419940	0.431339	6.60	6.44	6.36	42.7	24.5
$1^1B_g(3s)$	0.344115	0.423421	0.432983	6.36	6.34	6.32	42.6	39.2
2^1A_g	0.332172	0.411946	0.422615	6.68	6.65	6.60	22.0	23.1
$1^1A_u(3p_\sigma)$	0.333110	0.412507	0.423932	6.65	6.64	6.56	33.4	30.5
$2^1A_u(3p_\sigma)$	0.325782	0.405315	0.417249	6.85	6.84	6.74	38.0	22.5
$2^1B_u(3p_\pi)$	0.307771	0.392045	0.407016	7.34	7.20	7.02	66.2	76.0
CAS(4,5 + R1ex)-F								
1^1A_g	0.580375	0.660872	0.670545	0	0	0	21.6	21.8
1^1B_u(V)	0.339292	0.427612	0.440333	6.56	6.35	6.26	41.2	20.5
$1^1B_g(3s)$	0.347879	0.429877	–	6.33	6.29	–	42.5	–
2^1A_g	0.335032	0.416820	0.431189	6.68	6.64	6.51	22.0	26.2
$1^1A_u(3p_\sigma)$	0.336865	0.418951	–	6.63	6.58	–	33.4	–
$2^1A_u(3p_\sigma)$	0.329615	0.412012	–	6.82	6.77	–	37.9	–
$2^1B_u(3p_\pi)$	0.312068	0.399102	–	7.30	7.12	–	67.5	–

et al. [9] (Table 1). The $3p_\sigma$ Rydberg states (1^1A_u and 2^1A_u) are located at 6.56 and 6.74 eV [MR-AQCC/CAS(4,5 + R1ex)-R values in Table 7] and are assigned to the bands at 6.66 eV found experimentally by McDiarmid [2] and Doering and McDiarmid [3]. The transition to $2^1B_u(3p_\pi)$ at 7.02 eV [MR-AQCC/CAS(4,5 + R1ex)-R values in Table 7] is in good agreement with the value of 7.07 eV found by McDiarmid [2], Doering and McDiarmid [3] and Reddish et al. [9]. However, it should be noted that this transition had originally been assigned by Reddish et al. to ^1A_u in contrast to our assignment of ^1B_u. Our assignment is in agreement with previous EOM − CCSD$(T/\tilde{T})$ [10] and CASPT2 [11] results.

In the R1ex calculations the 1^1B_u state is significantly more diffuse [$< x^2 > \approx 43{a_0}^2$, CAS(4,5 + R1ex)-R] at the CI level than before. The MR-AQCC method corrects towards more valence character and restores the more pronounced valence character found in the three-state calculations. A slight overshooting by the MR-AQCC method is observed.

Conclusions

In the present work stable and systematic procedures for the balanced description of the lowest singlet excited valence and Rydberg states of butadiene, especially for the correct description of the 1^1B_u state, have been presented. Key roles are played by the orbital generation scheme CISD($\sigma\pi$-corr) and extended MR-CISD + Q/MR-AQCC calculations. Special attention was given to the 1^1B_u state as this is the most difficult state to describe. This difficulty was demonstrated, for example, by strongly varying results of CASSCF(4,4)-based calculations and a much larger sensitivity to extensions of the reference space and the basis set as compared with the 2^1A_g state. Starting with a CAS(4,4) reference space, we introduced systematic extensions of the reference space leading to a best computed excitation energy of 6.20 eV for the 1^1B_u state at the MR-AQCC level. Basis set extrapolations led to a further slight reduction to 6.18 eV. This is close to previous EOM − CCSD$(\tilde{T})$ [10] and CASPT2 [7, 11] results. In most previous calculations based on CI or CI-type methods significantly higher excitation energies were obtained [16, 17, 18, 19, 21], leading to significantly larger deviations from experiment. Our best value for the vertical excitation energy to the 2^1A_g state is 6.55 eV. This is below previous EOM-CCSD(T) and EOM − CCSD$(\tilde{T})$ calculations [10] by about 0.2–0.4 eV and demonstrates the deficiencies of these methods in the case of MR situations. On the other hand, the CASPT2 method [7, 11] gives an excitation energy of 6.27 eV, which is significantly too low.

The character of the 1^1B_u state is of valence character, with $< x^2 >$ values between $25.4{a_0}^2$ and $26.3{a_0}^2$ in the three-state calculations. In our calculations this state is even more compact than computed in previous investigations by Cave and Davidson [16] and by Cave [19]. Our $< x^2 >$ values are in good agreement with the EOM-CCSD(T) investigations by Watts et al. [10]. The valence character of the 1^1B_u state is strongly supported by calculations where Rydberg states, in particular the $2^1B_u(3p_\pi)$, are included. The clear separation of valence and Rydberg character is maintained in these calculations. The inclusion of size-extensivity effects at the MR-AQCC level is of particular relevance in this case.

Acknowledgements. The authors acknowledge support by the Austrian Science Fund within the framework of the Special Research Program F16 and project P14442-CHE and by the COST Chemisty/D26, project no. D26/0006–02. The calculations were performed mostly on the Schroedinger I Linux cluster of the Vienna University Computer Center.

References

1. Mosher OA, Flicker WM, Kuppermann A (1973) J Chem Phys 59:6502
2. McDiarmid R (1976) J Chem Phys 64:514
3. Doering JP, McDiarmid R (1980) J Chem Phys 73:3617
4. Hudson BS, Kohler BE, Schulten K (1982) In: Lim EC (ed) Excited states, vol 6. Academic, New York, p 1
5. Chadwick RR, Gerrity DP, Hudson DS (1985) Chem Phys Lett 115:24
6. Doering JP, McDiarmid R. (1981) J Chem Phys 75:2477
7. Ostojić B, Domcke W (2001) Chem Phys 269:1
8. Krawczyk RP, Malsch KM, Hohlneicher G, Gillen RC, Domcke W (2000) Chem Phys Lett 320:535
9. Reddish T, Wallbank B, Comer J (1986) 108:159
10. Watts JD, Gwaltney R, Bartlett RJ (1996) J Chem Phys 105:6979
11. Serrano-Andrés L, Merchán M, Nebot-Gil I, Lindh R, Roos BO (1993) J Chem Phys 98:3151
12. Hosteny RP, Dunning TH Jr, Gilman RR, Pipano A, Shavitt I (1975) J Chem Phys 62:4764
13. Buenker RJ, Shih S, Peyerimhoff SD (1976) Chem Phys Lett 44:385
14. Nascimento MAC, Goddard WA III (1979) Chem Phys 36:147
15. Nascimento MAC, Goddard WA III (1980) Chem Phys 53:251
16. Cave RJ, Davidson ER (1987) J Phys Chem 91:4481
17. Szalay PG, Karpfen A, Lischka H (1989) Chem Phys 130:219
18. Serrano-Andrés L, Sánchez-Marín J, Nebot-Gil I (1992) J Chem Phys 97:7499
19. Cave RJ (1990) J Chem Phys 92:2450
20. Lappe J, Cave RJ (2000) J Phys Chem A 104:2294
21. Cabrero J, Caballol R, Malrieu J-P (2002) Mol Phys 6:919
22. Kitao O, Nakatsuji H (1988) Chem Phys Lett 143:528
23. McMurchie LE, Davidson ER (1977) J Chem Phys 66:2959
24. Davidson ER (1996) J Phys Chem 100:6161
25. Müller T, Dallos M, Lischka H (1999) J Chem Phys 110:7176
26. Szalay PG, Bartlett RJ (1993) Chem Phys Lett 214:481
27. Szalay PG, Bartlett RJ (1995) J Chem Phys 103:3600
28. Shepard R, Lischka H, Szalay P G, Kovar T, Ernzerhof MJ (1991) J Chem Phys 93: 2085
29. Shepard R (1995) In: Yarkony DR (ed) Modern electronic structure theory, part I. World Scientific, Singapore, p 345
30. Lischka H, Dallos M, Shepard R (2002) Mol Phys 100:1647
31. Langhoff SR, Davidson ER (1974) Int J Quantum Chem 8:61
32. Bruna PJ, Peyerimhoff SD, Buenker RJ (1981) Chem Phys Lett 72:278
33. Dunning TH Jr (1989) J Chem Phys 90:1007
34. Kendall RA, Dunning TH Jr, Harrison RJ (1992) J Chem Phys 96:6769
35. Woon DE, Dunning TH Jr (1994) J Chem Phys 100:2975
36. van Mourik T, Wilson AK, Dunning TH Jr (1999) Mol Phys 96:529

37. Shavitt I (1977) In: Schaefer HF III (ed) Methods of electronic structure theory. Plenum, New York, p 189
38. Haugen W, Traetteberg M (1966) Acta Chem Scand 6:1726
39. Lischka H, Shepard R, Brown FB, Shavitt I (1981) Int J Quantum Chem Quantum Chem Symp 15:91
40. Shepard R, Shavitt I, Pitzer RM, Comeau DC, Pepper M, Lischka H, Szalay PG, Ahlrichs R, Brown FB, Zhao J (1988) Int J Quantum Chem Quantum Chem Symp 22:149
41. Lischka H, Shepard R, Pitzer RM, Shavitt I, Dallos M, Müller T, Szalay PG, Seth M, Kedziora GS, Yabushita S, Zhang Z (2001) Phys Chem Chem Phys 3:664
42. Lischka H, Shepard R, Shavitt I, Pitzer RM, Dallos M, Müller T, Szalay PG, Brown FB, Ahlrichs R, Böhm HJ, Chang A, Comeau DC, Gdanitz R, Dachsel H, Erhard C, Ernzerhof M, Höchtl P, Irle S, Kedziora G, Kovar T, Parasuk V, Pepper M, Scharf P, Schiffer H, Schindler M, Schüller M, Zhao J-G (2003) COLUMBUS, an ab initio electronic structure program, release 5.9
43. Dachsel H, Lischka H, Shepard R, Nieplocha J, Harrison RJ (1997) J Comput Chem 18: 430
44. Helgaker T, Jensen HJA, Jørgensen P, Olsen J, Ruud K, Ågren H, Andersen T, Bak KL, Bakken V, Christiansen O, Dahle P, Dalskov EK, Enevoldsen T, Heiberg H, Hettema H, Jonsson D, Kirpekar S, Kobayashi R, Koch H, Mikkelsen KV, Norman P, Packer MJ, Saue T, Taylor PR, Vahtras O (1997) DALTON, an ab initio electronic structure program, release 1.0
45. Bunge A (1970) J Chem Phys 53: 20
46. Halkier A, Helgaker T, Jørgensen P, Klopper W, Koch H, Olsen J (1998) Chem Phys Lett 286:243